FPCM-9 (2008)
The 9th International Conference on Flow Processes in Composite Materials
Montréal (Québec), Canada
8 ~ 10 July 2008

NON-CRIMP FABRIC PERMEABILITY MODELLING

S.P. Haanappel [1, 2], R. Akkerman [1]

[1] *Faculty of Engineering Technology, Chair of Production Technology, University of Twente, Drienerlolaan 5, P.O. Box 217 7500AE, Enschede, The Netherlands*
[2] *Corresponding author's Email: s.p.haanappel@student.utwente.nl*

SUMMARY: A qualitative study to the in-plane permeability modelling of Non-Crimp Fabrics has been carried out. A network flow model was developed to describe flow through inter bundle channels (meso level). To improve this model, it was extended with details that consider stitch yarn influenced regions. The model predicts a highly anisotropic permeability. The predicted permeability in the machine direction of the fabric corresponds with the experimental results. However, prediction of permeability perpendicular to the fabric's machine direction does not correspond with the experimental results. Possibly, flow through fibre filaments (micro level) is significant and the network flow model has to be extended to include this type of flow.

KEYWORDS: Non-Crimp Fabric (NCF), in-plane permeability prediction, network flow model, internal geometry, inter bundle channels, vacuum infusion

INTRODUCTION

Common problems that are encountered in Liquid Composite Moulding (LCM) processes are non-uniform impregnation, formation of dry spots, void inclusions and lengthy impregnation cycles. Accurate flow simulations are essential in finding the optimal process parameters. The infusion behaviour is strongly influenced by the fabric's permeability, which is inhomogeneous in case of a draped fabric. The permeability depends on the fabric's geometry, which is determined by positions and directions of fibres and yarns. This research focuses on the in-plane permeability prediction of Non-Crimp Fabrics (NCFs).

The main deformation mechanism during draping is shear, which influences the positions and directions of fibres and yarns. As a consequence, shear influences the fabric's permeability. A shear dependent geometrical description for the internal geometry of NCFs has been proposed by Loendersloot et al. [1,2]. For this, inter bundle channels were represented by Stitch Yarn induced fibre Distortions (SYDs). It was assumed that the flow through an NCF is mainly governed by flow through the inter bundle channels. Loendersloot [2] and Nordlund [4] developed a network flow model independently. Nordlund [4] analysed the flow in inter bundle channels by using a 3D flow model in Ansys CFX. The results served as an input for a network model. Loendersloot [2] represented the inter bundle channels (SYDs) by 1D finite elements (FE), to be assembled in a network model as well. Model results and experiments [2] did not correspond well. Therefore, this model will be extended with elements that describe stitch yarn related regions.

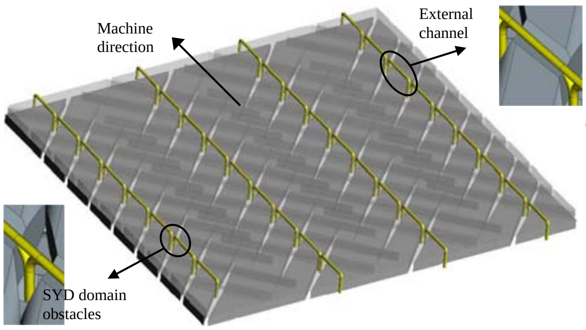

(a) One layer NCF, consisting of 2 plies. The upper ply is transparent, such that the intersections of SYDs in the upper ply with the lower ply can be seen.

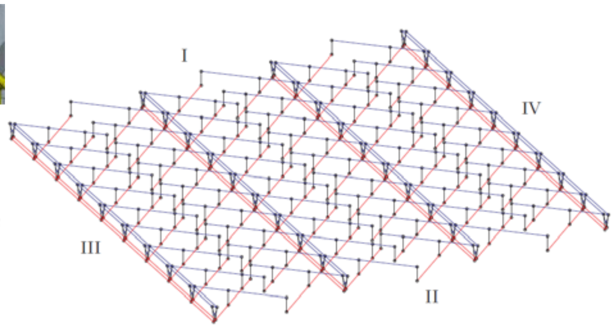

(b) Elemental representation of the piece of NCF in Fig. 1(a).

Fig. 1 Piece of unsheared biaxial NCF, characterised by stitch distances 3*A* and 9*B*.

NETWORK FLOW MODEL

The FE formulation for a 1D element was obtained by using the continuity equation for an incompressible slow viscous flow, after which a weak formulation was applied. Darcy's law for one spatial dimension was used as a constitutive equation:

$$\Phi = -\frac{AK}{\mu}\frac{\mathrm{d}p}{\mathrm{d}x}, \tag{1}$$

in which the terms Φ, A, K, μ, p and x represent volume flow, cross sectional area, permeability, viscosity, pressure and one Cartesian coordinate, respectively. Subsequently, assuming a linearly varying pressure over an element and choosing the pressure interpolation function equal to the element shape function, results in the following expression for a 1D element:

$$\frac{AK}{\mu L}\begin{bmatrix} 1 & -1 \\ -1 & 1 \end{bmatrix} \cdot \vec{p} = \vec{\varphi}, \tag{2}$$

in which $\vec{p}$, $\vec{\varphi}$ are the nodal pressure and nodal flux vector, respectively. A network can be created by connecting 1D elements, which results in a global system:

$$\underline{M} \cdot \vec{p} = \vec{\varphi}, \tag{3}$$

with $\underline{M}$ the system matrix. Fig. 1(b) shows an elemental representation of a piece of NCF.

FLOW DOMAIN

Particular regions in the NCF are considered to be a part of the flow domain. These regions can be described by 1D elements (Eqn. 2). Finally, the elements may be assembled in a system (Eqn. 3) that represents a piece of NCF. The considered flow domains in the NCF in Fig. 1(a) are:

- The wedge shaped channels (SYDs). SYDs in the upper ply intersect SYDs in the lower ply and form continuous channels. Fig. 2 shows these intersections schematically, characterized by intersection distances *D*.
- The region where the stitch yarns penetrate the fabric, magnified in the lower left corner of Fig. 1.
- The regions next to the stitch yarns, which run from one stitch yarn penetration point to the other stitch yarn penetration point (magnified in the upper right corner in Fig. 1(a)).

Stitch Yarn Induced Fibre Distortions

The connection and number of connections of intersecting SYDs depend on stitch yarn penetration positions at $(a+j\ ,\ b+k)$, stitch distances *A* and *B*, SYD lengths l^l and l^u and the fibre filament directions θ^l and θ^u, see Fig. 2. The superscripts *l* and *u* correspond to the lower and upper ply respectively. At the intersection points, nodes have to be assigned. Continuous regions in SYDs between those nodes can be described by a 1D element (Eqn. 2).

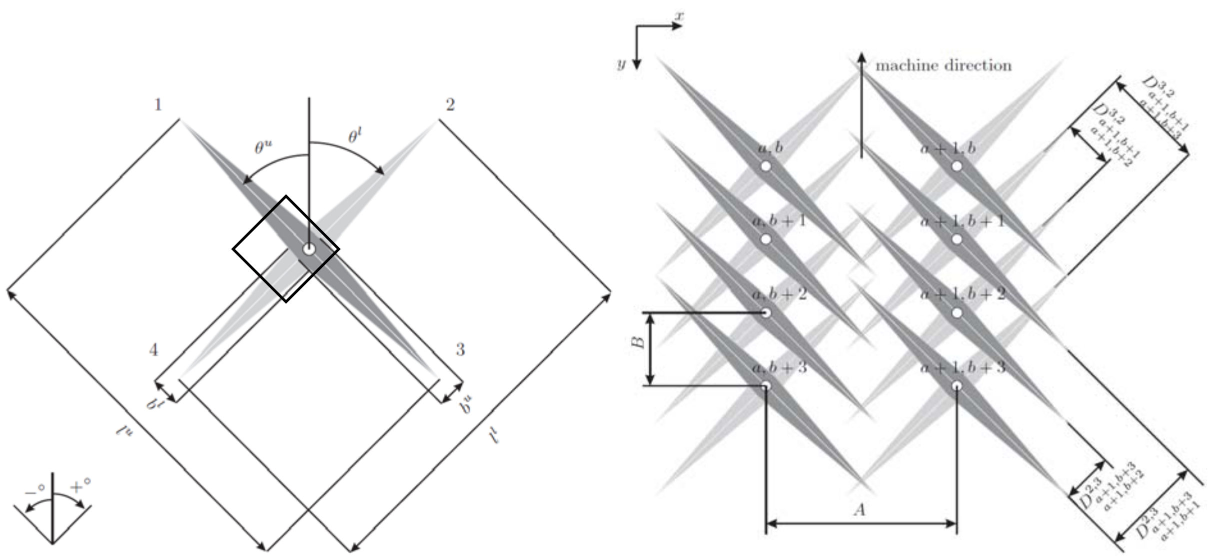

(a) SYD pair of a bi-axial NCF, consisting of a SYD in the lower and upper ply. SYD arms are numbered from 1 till 4. The region within the rotated square is represented in Fig. 3c.

(b) Stitch yarn penetration points at (a+j,b+k) for an unsheared piece of NCF.

Fig. 2 The SYD arms intersect each other at intersection distances *D* in which sub and super scripts refer to associated penetration points and the SYD arm number respectively.

The effective permeability *K* of an element, will be the effective permeability of its representing part of the SYD. Fig. 3(a) shows a part of a SYD, which is assumed to be a wedge shaped channel with a constant height *h*. It could be considered as an infinite amount of serially connected channels of length dx with a spatial dependent cross sectional area $A(x)$, such that the effective permeability K_E of this channel can be determined with [2]:

$$K_E = L\left(\int_0^L \frac{1}{K(A(x))}\mathrm{d}x\right)^{-1} \tag{4}$$

Results from Mortensen et al. [3] were used to describe the permeability for the spatial dependent cross section of the channel. These are relations for the hydraulic resistance of channels with a rectangular cross section, dependent on the compactness. The compactness is related to the perimeter and the area of the channel’s cross section.

SYD Domain Obstacles

The magnified region in the lower left of Fig. 1(a) shows a stitch yarn that penetrates the fabric. The stitch yarns in a SYD disturb the flow and could influence the overall permeability significantly. This region can be described by the domain in figure Fig. 3(c), where four opening surfaces are numbered from 1 till 4. Each opening represents the connection with the SYD-arms (Fig. 2(a)).

The connections between the openings 1 till 4 can be described by the assembly of six 1D elements (Eqn. 2), as is shown in Fig. 3(d). The elements describe all possible connections between the openings. They contain an individual permeability, so that each direction has a particular flow resistance. The permeability values were determined in a parametrical study using Ansys CFX, for varying dimensions b, d_c, and h.

External Channels

The magnified region in the upper right of Fig. 1(a) shows a stitch yarn, which runs from one stitch yarn penetration point to another stitch yarn penetration point. When the NCF has been positioned between rigid mould parts, the compression mechanism pushes this stitch yarn in the fabric. As a result, a channel will be created on both sides of this stitch yarn and can be described by a 1D element (Eqn. 2). The cross sectional geometry of the channel in Fig. 3(b) has been idealised in order to perform a parametrical study.

It has been assumed that the cross sectional area is constant over the element's length and that pushing the stitch yarn in the fibrous ply could lead to deformation of the stitch yarn's cross section. This leads to an elliptical cross section with major axis $2e$ and minor axis $2f$. Again, permeability values were determined in a parametrical study using Ansys CFX, for varying dimensions e, f and g.

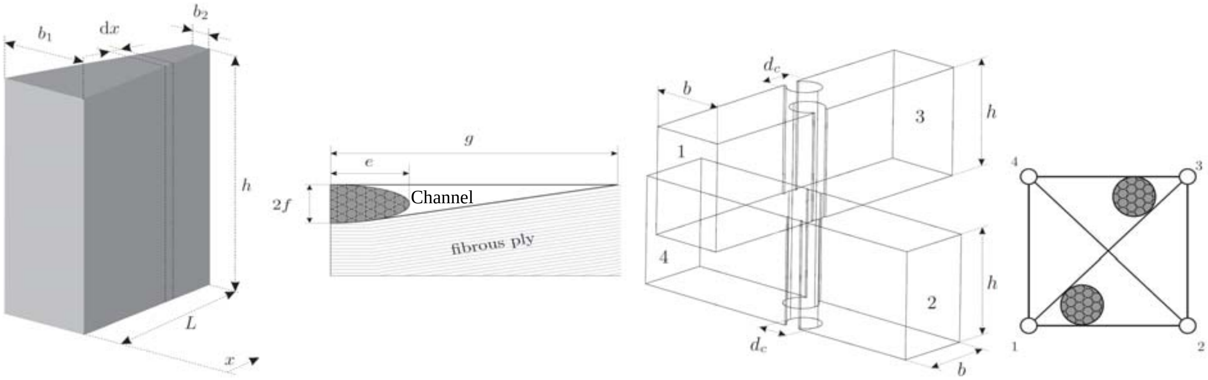

(d) Channel with linear varying width (SYD). *(a) External channel, created by pushing the stitch yarn in the fabric.* *(c) Flow domain around the penetrating stitch yarn.* *(b) 1D elemental representation of Fig. 3(c).*

Fig. 3 Flow domains for which individual permeability relations were determined.

MODEL IMPLEMENTATION

The network flow model was obtained by assembling all elements that describe the different flow domains, with a typical result depicted in Fig. 1b. The properties of the fabric under consideration are listed in Table 1.

Table 1 Properties of the biaxial NCF that was used for the infusion experiments

manufacturer		Devold
areal density ρ_A	[kg·m^{-2}]	0.541
fibre		Tenax HTS 5631
fibre count in tow	[-]	12K
fibre material		carbon
fibre density ρ_f	[kg·m^{-3}]	1750
orientation	[°]	∓45
stitch		PES
linear density	[tex]	5
stitch yarn diameter d_c	[mm]	0.071
knit pattern		chain
stitch distance A according to [2]	[mm]	5.71± 0.04
stitch distance B according to [2]	[mm]	2.20± 0.02

To determine the permeability of the fabric in the machine direction, a pressure difference was created by applying boundary conditions at the sides I and II (Fig. 1b). To determine the permeability of the fabric perpendicular to the machine direction, a pressure difference was created by applying boundary conditions at the sides III and IV (Fig. 1b). For the internal domain, nodes fulfil the restriction $\varphi = 0$. Once the system is solved for the unknown pressures, the effective permeability can be determined with:

$$K_E = \frac{\mu \overline{L}}{A \Delta p} \sum \varphi_h \qquad \text{or} \qquad K_E = \frac{\mu \overline{L}}{A \Delta p} \sum \varphi_l \tag{5}$$

in which $\overline{L}$ is the length between sides with low and high pressure boundary conditions, Δp the pressure difference between the applied high and low pressure and summation will be done over all nodal fluxes φ, at nodes with high pressure boundary conditions or nodes with low pressure boundary conditions. The cross sectional flow area A is determined by $V / \overline{L}$, in which V is the total volume of the elements, i.e. the volume of the inter bundle channels.

Results

The model was solved several times, in which the fabric's height *2h* (twice the height of a SYD in case of a biaxial NCF) and the maximum width *b* of the SYDs (Fig. 2a) were varied. The SYD lengths *l* were 8, 1 [mm]. The dimensions of the external channels were determined by microscopic analyses and were processed in the model.

The results in Fig. 4 show that the permeability is very dependent on the width of the SYDs. The height of the fabric influences the permeability less. This height is related to the height of the SYDs. The height *h* of the wedge shaped channel in Fig. 3a influences its effective permeability less, compared to the channel's widths *b*. Since the SYDs influence the effective permeability of the fabric much, this behaviour is seen at this scale as well.

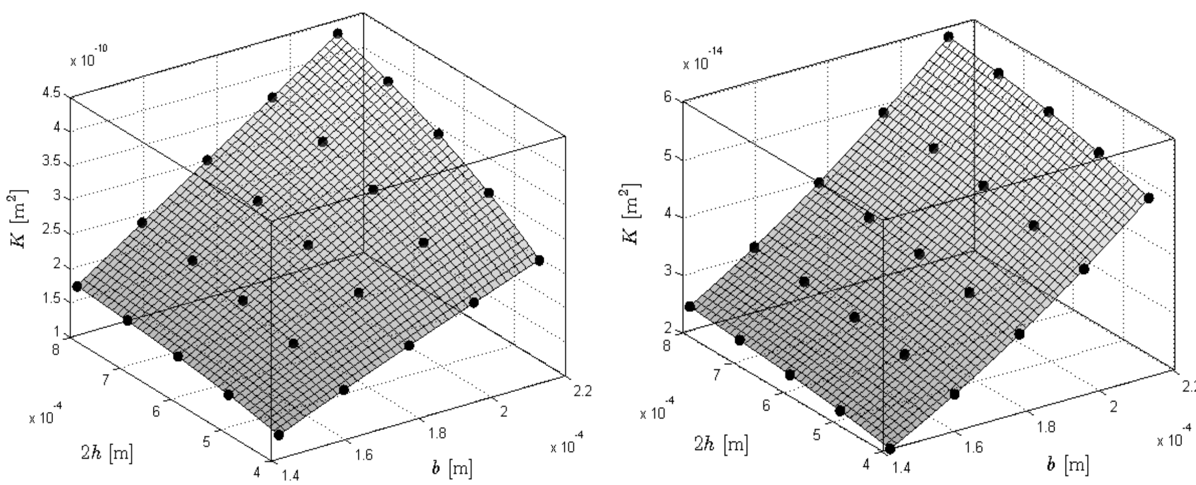

(a) Pressure gradient direction in the fabric's machine direction.

(b) Pressure gradient direction perpendicular to the fabric's machine direction.

Fig. 4 Results of a network as in Fig. 1b with the dimensions 10*A* and 25*B* (Fig. 2b).

The model predicts a highly anisotropic permeability. Comparing Fig. 4a with Fig. 4b, the anisotropy is characterised by a difference of four orders of magnitude. The predicted anisotropic character is mainly caused by the SYD intersection points, which are more ideally located for infusion in the machine direction (Fig. 2b). The orientation of the elements that describe the external channels (Fig. 1 and Fig. 3b), influences the anisotropy as well.

EXPERIMENTAL VALIDATION

To validate the network flow model, liquid infusion experiments were performed. A simple vacuum infusion set-up was developed. The set-up roughly consists of two glass plates, within between the fabric to be infused (Fig. 5) with a viscous, Newtonian and incompressible liquid (maple syrup). To seal the infusion domain, tacky tape has been positioned around the infusion domain, after which a transparent foil was trimmed over the upper glass plate. The pressure difference was created by attaching a vacuum pump at the outlet tube.

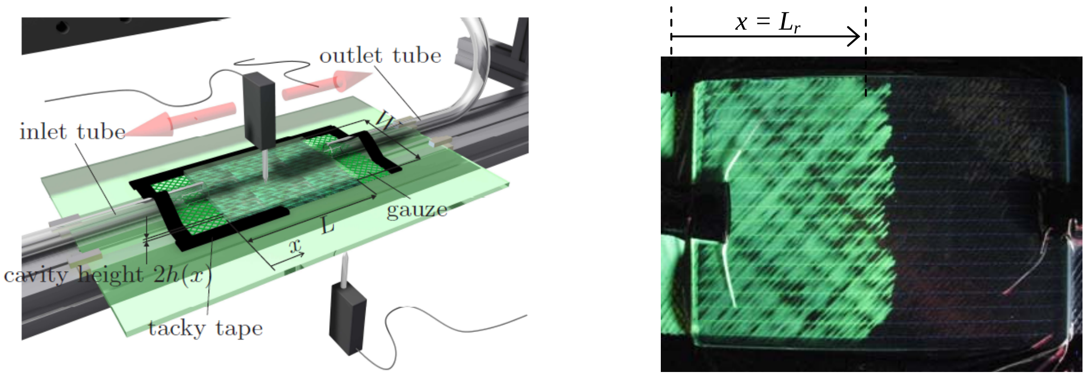

(a) The fabric was infused between two glass plates.

(b) Flow front and its position, visualized by using a fluorescent.

Fig. 5 Experimental set-up.

Since no spacer or clamping system was used, the cavity height varies along the infusion direction. Since the fibre volume fraction is dependent on the cavity height $2h(x)$ and thus on the permeability, the cavity height was measured during the experiments by using two height sensors. A formulation, based on serially connected permeabilities was used to determine the effective permeability at the flow front position $x=L_r$ (Fig. 5b):

$$A_E K_E\big|_{x=L_r} = L_r \left(\frac{L_r - \Delta x}{A_E K_E\big|_{x=L_r-\Delta x}} + \frac{\Delta x}{A_E^{\Delta x} K_E^{\Delta x}} \right)^{-1} \tag{6}$$

with the following effective cross sectional areas:

$$A_E(L_r) = \frac{1}{L_r}\int_0^{L_r} A(x)\mathrm{d}x \qquad A_E(L_r - \Delta x) = \frac{1}{L_r - \Delta x}\int_0^{L_r-\Delta x} A(x)\mathrm{d}x \qquad A_E^{\Delta x} = \frac{1}{\Delta x}\int_{L_r-\Delta x}^{L_r} A(x)\mathrm{d}x \tag{7}$$

Repeatedly applying Eqn. 6 for every flow front position L_r with a resolution that is determined by Δx, results in a position dependent permeability. Different relations for K_E were used, i.e.:

$$K_E(L_r) = \left. \frac{\Phi \mu L_r}{A_E \Delta p} \right|_{x=L_r} \tag{8}$$

for which it was assumed that a steady state (Eqn. 1) situation for every flow front position L_r was obtained. Another relation is based on the flow front position L_r and its associated infusion time:

$$K_E(L_r) = \left. \frac{\mu L_r^2}{2t\Delta p} \right|_{x=L_r} \tag{9}$$

Only results that were obtained by combining Eqn. 6 and Eqn. 9 are shown in this paper (Fig. 6). All variables in Eqn. 8-9, were acquired by sensors during the infusion experiments.

Results

For each fabric orientation (infusion in the machine direction and infusion perpendicular to the machine direction), three reliable experiments were executed. Fig. 6 shows the results, in which a shaded area with a single colour refers to one particular experiment. During the infusion experiments, the cavity height was time dependent as well. Therefore, the permeability determinations for one experiment were done by using the initial cavity 2 $h(x,t=T1)$ and the final cavity 2 $h(x,t=T2)$, which are characterised by open en filled markers respectively in Fig. 6. The permeability $K(x)$ as a function of the fabric's position x was obtained by using Eqn. 6. The $K(h)$ plots in Fig. 6 were obtained by combining $K(x)$ and 2 $h(x)$.

The figures show a slightly increasing permeability, as the fabric's height increases (for a decreasing fibre volume fraction). The variation between the different experiments and the time dependent cavity height are the sources of the scatter. However, these results indicate in which order range, permeability values of this biaxial NCF lie. Comparing Fig. 6a and Fig. 6b, the fabric's permeability is nearly isotropic.

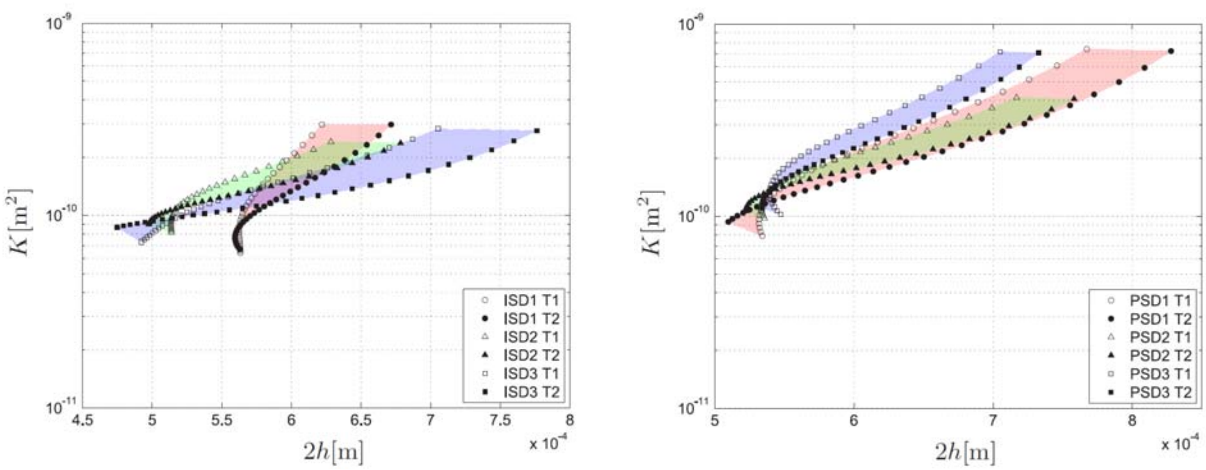

(a) Pressure gradient direction along the fabric's machine direction.

(b) *Pressure gradient direction perpendicular to the fabric's machine*

Fig. 6 Results from infusion experiments determined by using Eqn. 6 and Eqn. 9.

CONCLUSIONS

The network flow model proposed by Loendersloot [2] was extended by including stitch related features. The network flow model predicts an anisotropic permeability, while infusion experiments show an isotropic permeability. However, for the experiments with infusion in the machine direction, Fig. 4a and Fig. 6a show good agreement in permeability values (considering the order of magnitude).

Since the network flow model is based on flow through inter bundle channels, the predicted anisotropy of the permeability and the isotropic permeability from the experiments, indicate that flow between the fibre filaments (at micro level) is significant. Therefore, it is needed to extend the network flow model, to account for this type of flow.

The model predicts that the effective permeability depends strongly on the micro geometry, in particular on the width of the SYDs. Therefore, when varying the fabric's height, it is necessary to relate the network model to compaction mechanisms of an NCF that could describe the dimensions of the SYDs. Some work [1, 2] was already done, which related the size of the stitch yarn and the shear angle of the fabric to the SYD dimensions.

REFERENCES

1. R. Loendersloot, S.V. Lomov, R. Akkerman and I. Verpoest, "Carbon Composite based on Multiaxial Multiply Stitched Preforms. Part V: Geometry of Sheared Biaxial Fabrics", *Composites Part A*, Volume 37, pages 103–113 (2006).

2. R. Loendersloot, "The Structure–Permeability Relation of Textile Reinforcements", *PhD thesis*, University of Twente (2006). ISBN 90-365-23337-0.

3. N.A. Mortensen, F. Okkels and H. Bruus, "Reexamination of Hagen-Poiseuille Flow: Shape Dependence of the Hydraulic Resistance in Microchannels", *Physical Review E*, Volume 71, Number 057301 (2005).

4. M. Nordlund, "Permeability Modelling and Particle Deposition Mechanisms Related to Advanced Composites Manufacturing", *PhD thesis*, Leleå University of Technology (October 2006).